Merged AMSR-2 and GPM Passive Microwave Radiometry for Measuring River Discharge and Runoff

G. Robert Brakenridge[1]
Son. V. Nghiem[2]

[1]University of Colorado, USA, [2]JPL, California Institute of Technology, USA

Accepted, IEEE, Selected Topics in Applied Earth Observations and Remote Sensing, special issue "Contributions to Global Water Cycle Science and Applications from GCOM-W/AMSR2, 2017

Abstract

River discharge and runoff have long been measured on the ground at *in situ* gauging stations, but today's global hydrologic models require improvements to the quantity and quality of such observational information. Satellite remote sensing of the Earth's water cycle has only recently been extended to measurements of discharge. We demonstrate that passive microwave radiometry has a surprising power to monitor river discharge changes at an appropriate temporal sampling interval (daily) and with considerable accuracy, over multiple decades and continuing into the future. This capability was unanticipated as the AMSR-2, AMSR-E, and the TMI and GMI sensors were being designed. However, their ~37 GHz data are now being used to provide important river discharge and runoff information commencing in 1998. Such observational data can be used to address important science issues, such as the effects of climate change on arctic river freshwater discharge, and associated dissolved organic matter and heat fluxes into the Arctic Ocean.

Introduction

Because of its importance to local economies, river discharge and runoff have long been measured on the ground at gauging stations [1]. However, the river data are not freely shared among all nations, and each station requires a sustained investment even after installation has been completed to maintain its calibration to discharge. Even though many river basins are transnational, efforts to compile data internationally are only partially successful. This type of water data is regarded by some nations as state secrets; in other parts of the world, data collection is reduced due to funding issues [2]. At some locations, it has never been initiated (figure 1). As a result, the measurement needs and how they may be addressed are active topics of discussion in the hydrological community [1, 3].

Accurate hydrological modeling also depends critically on improvements to the observational data: "processing more of the same poor quality data will only lead to poorer quality model results" [4]. Satellite-based measurements of the Earth's water cycle are therefore central to better understanding surface water fluxes and to modeling thereof [5]. These observations are required for more efficient water resources management and better prediction of and responses to floods and droughts [6, 7]. Work on atmospheric components of the water cycle has made rapid progress: with the advent of satellite precipitation and groundwater storage measurements at continental to global scales. The fluxes of

water to and from the Earth's surface and its atmosphere are, increasingly, being directly measured. Now, another critical

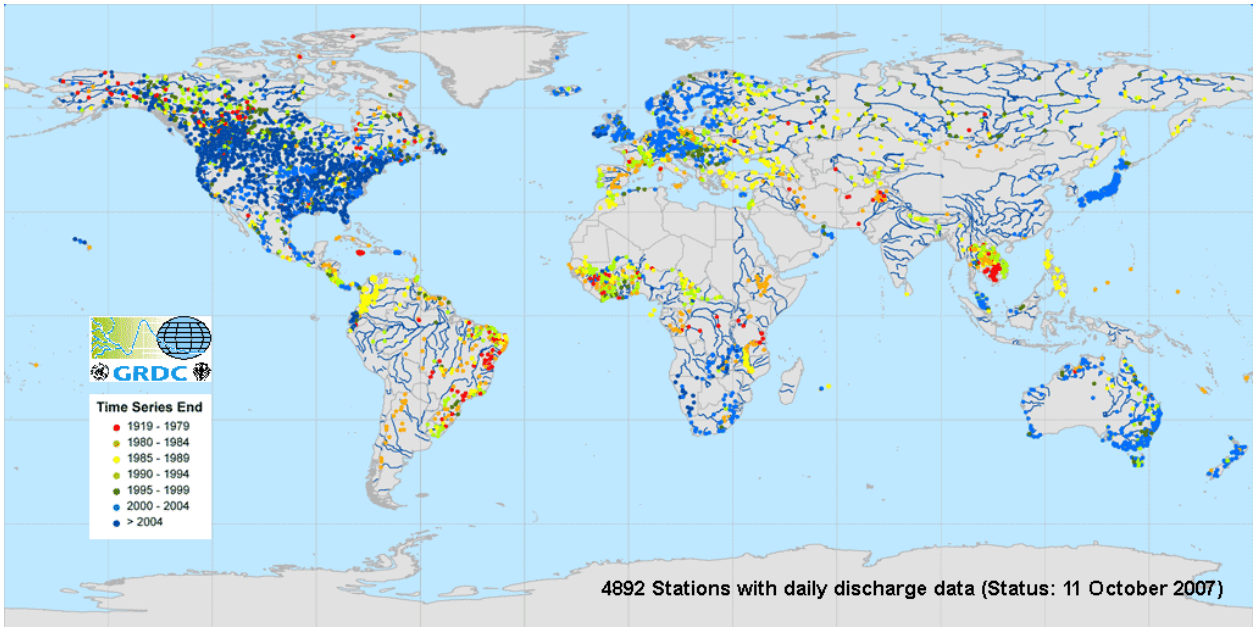

Figure 1. River discharge gauging stations with records collected at the Global Runoff Data Centre (GRDC). Only blue stations are currently active; others discontinued. Mainly only monthly data are available from GRDC; archives of daily data are much more limited. Coverage is exceptionally sparse in much of South America, southern Africa, and Asia [8].

component of the cycle, *water surface runoff* (in mm) and *river discharge* (in m3/s), is beginning to be measured via remote sensing. We address here one method to accomplish such direct measurement.

Definition of Discharge and Runoff

River and stream watersheds are defined in map view by the surface drainage network. Watersheds generate river base flow (during times of no precipitation or snowmelt) from groundwater discharge. The visible rivers, lakes, and wetlands in a watershed are the surface water expression of that ground water system. Also, during and after precipitation events or periods of snowmelt, higher runoff amounts and discharge are achieved for various lengths of time (referred to as storm or flood hydrographs). *Discharge* (equation 1) is the volume of channeled water moving pass a measurement site along a river, expressed as

Equation 1 $Q = wdv$

Q is discharge in m^3/s, w and d are flow width and depth, respectively, in m, and v is flow velocity in m/s.

Discharge is commonly measured on the ground via continuous river level (stage) recording, and then calibrated to discharge by intermittent sampling of the cross-sectional flow area and flow velocity (current velocity meters are lowered into the river). Intermittent

measurements of Q, by field measurements of flow cross sectional area and velocity, provide information about Q at different d (measured in the field as stage) values. The relation between Q and stage is known as a rating curve, and it must be revised over time as channel dimensions, and thus the actual empirical relation, change. However, once established, instantaneous discharge is commonly measured to ±20% using only the stage value.

Runoff is essentially the same information, but adjusted to watershed area and particular time intervals. Thus, an average discharge in m^3/s measured for the day, via stage, can be immediately transformed to total daily water volume/day using the total number of seconds in a day. This daily volume is usefully recast to daily runoff by dividing volume by total upstream drainage area.

Equation 2 $R = 86400 \times Q/A$

Where R is runoff in mm/day, Q is discharge converted to mm^3/s, and A is contributing watershed area, in mm^2

Among the uses of this conversion from Q to R is that R is directly comparable to other relevant measurements or model results for watershed land surfaces, such as total mm of daily rainfall or evapotranspiration. Note that these units are conventionally used in hydrology, rather than the International System of Units.

Temporal Sampling Requirements

In the latter part of the 20th century, it was widely believed in the remote sensing/Earth Science community that discharge and runoff could not be directly measured from orbital platforms, but must instead be either modeled, or measured on the ground. There are two reasons for this:

1) Flow velocity is critical in any direct measurements of discharge (per equation 1), and, so far, there are only very experimental techniques of retrieving even surface flow velocities; direct measurements of cross sectional flow velocities from remote sensing are not available at all.

2) Although, in principle, accurate river stages can be measured via satellite altimetry, discharge along many rivers can vary by an order of magnitude over time scales of only several days (Figure 2). An altimetric satellite system capable of retrieving stages on a global basis at this temporal resolution is difficult to accomplish. Like precipitation, runoff can be a very dynamic phenomenon, and difficult to adequately characterize unless revisits of daily or at least near-daily can be attained.

In this regard, NASA's upcoming Surface Water and Ocean Topography Mission (SWOT) will offer, for the planned mission duration of ~3 years, river stage data at many locations across the world on a relatively coarse time step (weekly or twice-weekly, depending on latitude), but with a high precision of several cm. A major use of such data will be calibration of hydrological models which produce river stage and slope results along extensive drainage networks or even globally [9]. The calibrated models can then, in turn, be driven with daily climatology to predict river discharge and runoff at similar time steps. SWOT will be the first altimetry mission designed to monitor discharge and runoff changes, but its temporal sampling and limited

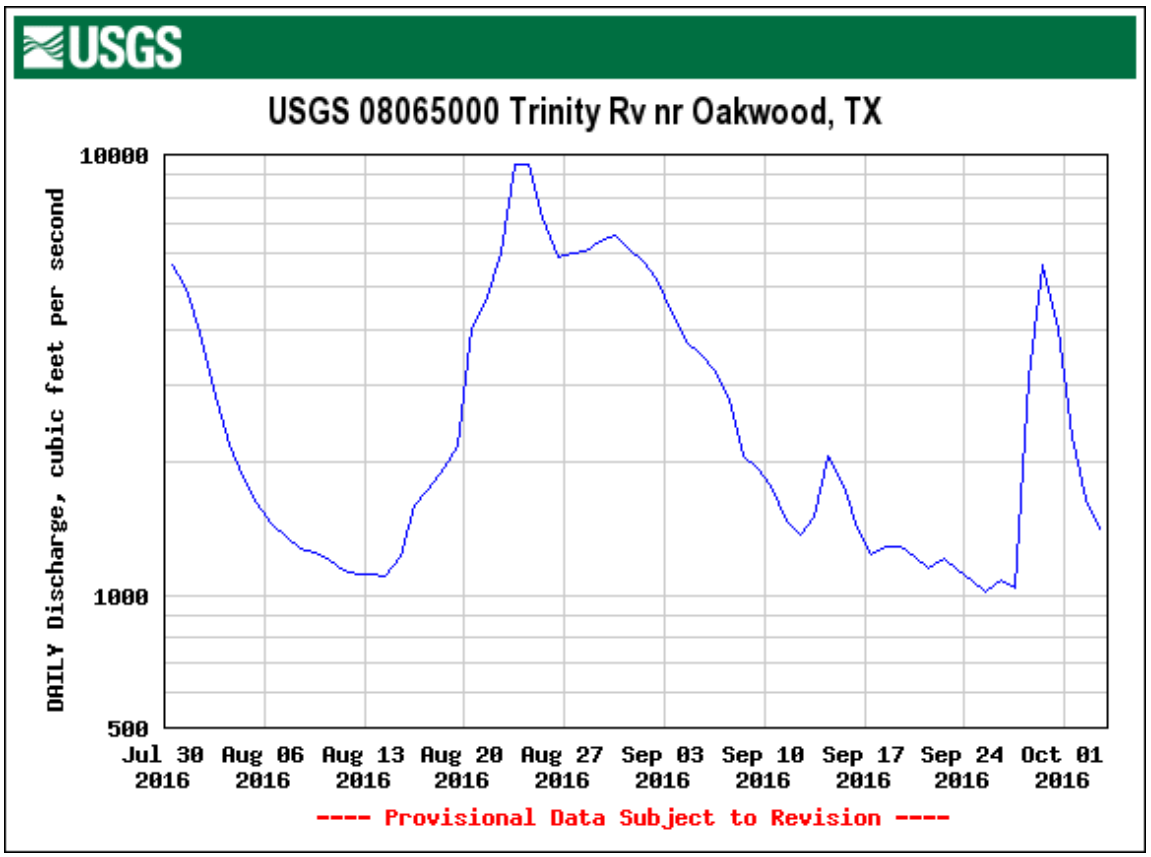

Figure 2. Portion of the gauging station discharge record for the Trinity River, Texas. In late September, 2016, discharge rose from ~1000 ft^3/s to ~ 5000 ft^3/s in three days. In August of the same year, an order of magnitude increase occurred in 8 days.

mission duration constrain its utility for sustained observations. Our work demonstrates, however, that satellite microwave radiometry technology has the ability to measure discharge and runoff with the advantage of a daily record extending back to at least 1998, and continuing indefinitely into the future, for as long as satellites such as GCOM-W, GPM, and follow-ons continue to operate. The radiometry method does require accurate calibrations, which can be provided by river gauging, or in the future by SWOT measurements, thereby extending the value of SWOT extensively in time and in space over the world. Where there is no river gauge or SWOT coverage, the calibration can be accomplished by using a hydrology model such as the Water Balance Model (WBM) to estimate river discharge within the limit of model uncertainties [10, 11].

Potential of Microwave Radiometry

Satellite microwave sensors such as carried aboard GCOM-W and GPM provide global coverage of the Earth's land surface on a daily basis and, at certain wavelengths, without major interference from cloud cover. Using a strategy first developed for wide-area optical sensors [7], these sensors (e.g. AMSR-E, AMSR-2, TRMM, and GPM) can measure river discharge changes via the accompanying changes in reach surface water extent. As rivers rise and discharge

increases, water area within “satellite gauging sites” (selected parcels of floodplain land measuring approximately 10 km x 10 km; figures 3-5) also rises [10, 12].

The parcels are selected from globally gridded microwave products whose pixels are at this spatial scale. A ~37-GHz image pixel of these dimensions centered over a river is commonly "mixed"; it includes both water (low emission), and land (much higher emission). As the proportion of water area rises, the bulk emitted radiation declines. The microwave signal is thereby sensitive to flow width changes (figure 6).

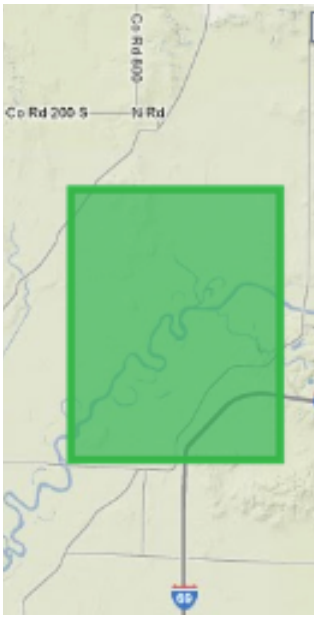

Figure 3. Footprint of a ~10 km measurement pixel from a daily global gridded microwave product produced at the JRC. This pixel is a measurement site for monitoring discharge changes along the Wabash River, southern Indiana, U.S.

With *in situ* river gauging stations, transformation of the remote sensing signal to river discharge values must be accomplished using a rating equation.

Figure 4. A meander bend within the measurement pixel showing the opportunity for flow area expansion onto the point bars and floodplain as stage and discharge increase.

Figure 5. Ground view of a typical river meander, showing the point bar (inside of meander bend) and steeper cut bank (outside of bend). As flow increases, flow width and measurement site water area increase.

For an automated online satellite-based system (River Watch), http://floodobservatory.colorado.edu/Di

schargeAccess.html), the calibrating discharge values are instead obtained by runs of a global runoff model [10, 12]. Five years (2003-2007) provide abundant model output for calibration. The model produces daily discharge values for these years at each measurement site and we use daily maximum, mean and minimum values for each month of the 5-year period (model global grid resolution is also 10 km). A rating curve equation then is constructed from the set of 180 daily discharge/remote sensing pairs (figure 7). Commonly, the equation is either linear or a second-order polynomial "best fit." As for in situ stage/discharge rating equations or curves, the relations are entirely empirical.

The potential for remote sensing of streamflow is demonstrated in figures 6 and 7 (daily values) and 8 (monthly runoff). The use of *in situ* data provides the best rating equation, but even the model-derived curve, though exhibiting a different slope, allows for useful results without the need for data from the ground. The model predictive strength is assessed by Nash-Sutcliffe statistics [13], discussed in a section below.

Significant scatter is expected in model/remote sensing plots of daily values, as both model and remote sensing errors are included. In this regard, global scale modeling may perform poorly at some sites in simulating daily discharge changes, even while the remote sensing is tracking actual discharge and runoff

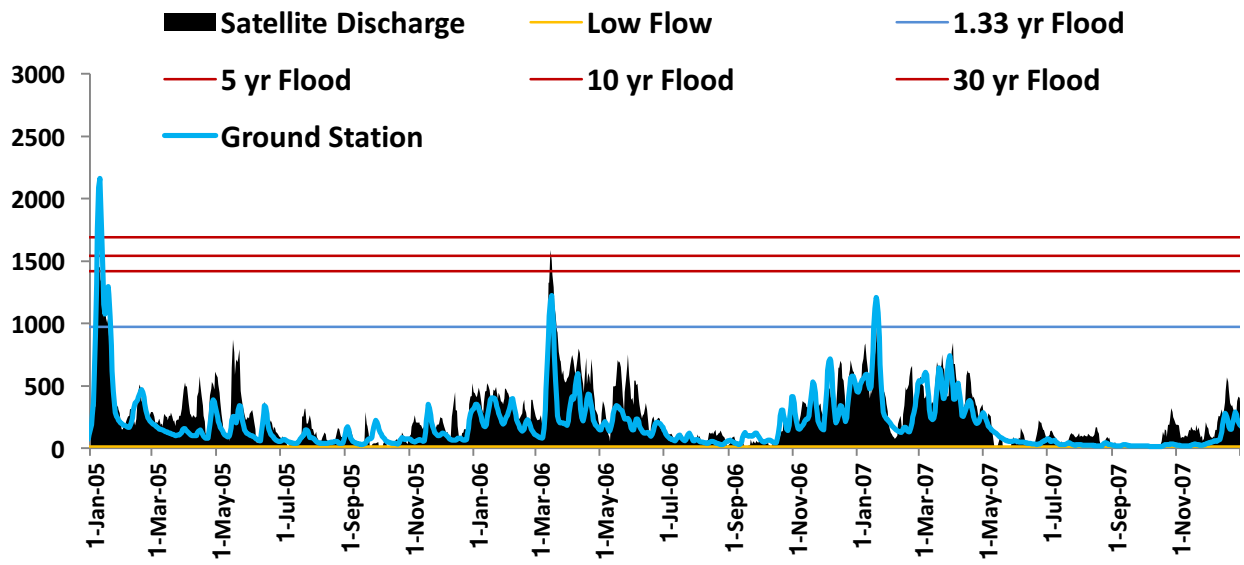

Figure 6. *In situ* gauging station information (blue line) can be compared with the satellite water flow area signal for co-located measurement sites/gauging stations in the U.S. In this example for River Watch site 446, Trinity River, Texas, the two independent time series of station data (blue line) and remote sensing (black) are shown for a portion of the 1998-present period of record. The satellite-based flow area measurements have been first transformed to discharge values using an empirical regression equation (Figure 7).

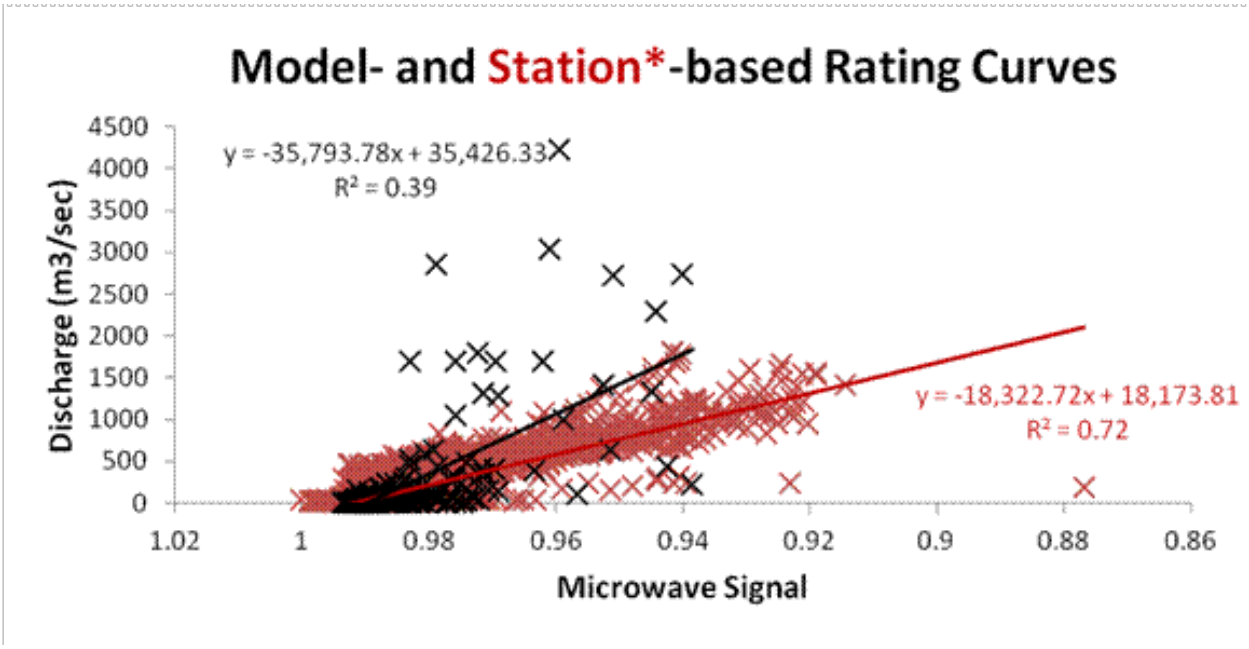

Figure 7. Two rating equations for site #460, Trinity River, Texas. The WBM model results are shown as black crosses, and exhibit a large amount of scatter compared with the remote sensing. The scatter is expected because the river includes control structures that are not part of the WBM model. The *in situ* gauging station discharges are more highly correlated to the remote sensing.

changes very well (figures 6-8). Or the site may be poorly located and the remote sensing signal itself not be very sensitive to discharge changes (e.g., rivers within narrow mountain valleys). However, in many cases, at sites where discharge causes significant changes in surface water area, there is a strong correlation between modeled discharge and the remote sensing signal: both are independently tracking actual discharge changes (figures 9 and 10).

We have obtained hundreds of rating curves, globally, similar to that in figure 9; but more work remains in order to improve the results: a) the straight line rating illustrated in figure 9 is a simplistic fit to the data, b) the amount of scatter appears to decrease with increasing discharge, and c) attempts to calculate a daily confidence interval or error limits for daily values must consider that these will vary for low flow and high flow states (figures 8 and 9).

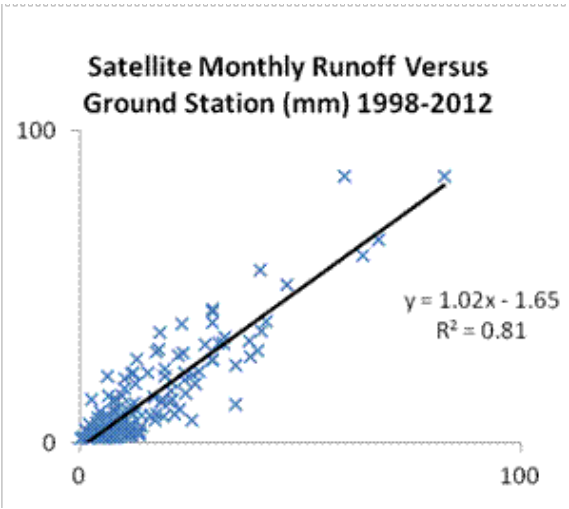

Figure 8. Satellite observation of Trinity River monthly runoff at River Watch site #460, compared to runoff measured at the local gauging station.

For most River Watch sites at present, there is no comparison to *in situ* data, and if the WBM model exhibits bias, this will be reflected in the rating curve and in the satellite-based daily discharge values. However, we stress that the observed model/remote sensing scatter in plots such as figure 9 does not necessarily represent errors in microwave signal or limits to the accuracy of the method, but instead is likely induced by model errors; this is known to be the case for a number of rivers monitored by in situ gauging stations in the U.S. (figure 7).

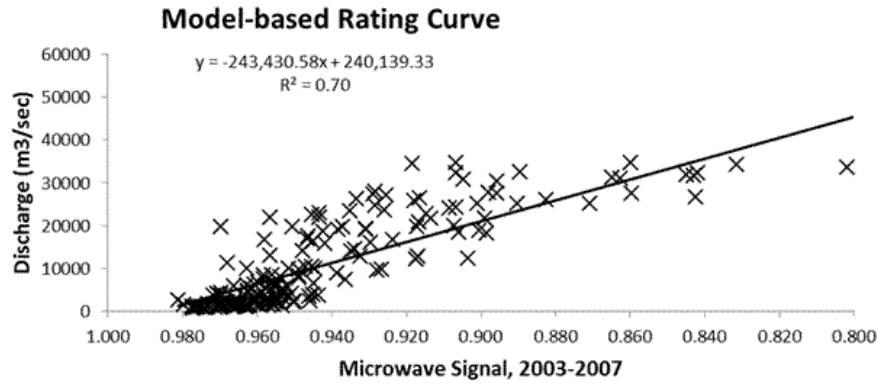

Figure 9. Scatter plot comparing WBM-modeled daily discharge over a 5-year period (January-December monthly daily maximum, minimum, and mean discharges) to the remote sensing for River Watch site #30 along the Ayeyarwady River, Myanmar. Although a better curve could be fit to these data, a straight line is a useful first-approximation rating curve.

River Watch Data Processing

River Watch version 3 and higher (figure 10) uses the NASA/Japanese Space Agency Advanced Scanning Microwave Radiometer AMSR-E band at 36.5-GHz, the NASA/Japanese Space Agency TRMM 37 GHz channel, and 37-GHz information from the AMSR-2 and GPM sensors. The discharge estimator (the remote sensing signal) is the ratio of the daily calibrating value ("C") that represent the 95th percentile of the day's driest (brightest) emissivity within a 9 pixel x 9 pixel array surrounding the site, and "M", the emissivity from a measurement pixel centered over the river and its floodplain. The 95th percentile is used instead of the hottest pixel to exclude outliers due to measurement noise.

Passive microwave signatures measured by a radiometer over a target area are related to the product ($T \times e_H$) of the physical temperature T and surface emissivity e_H for the horizontal polarization H [10, 13]. Thus, the signatures at both the calibration target C and the measurement target M vary with the land surface temperature that drives the seasonal rhythm of the landscape. Unlike the polarization ratio or gradient ratio traditionally used in passive microwave remote sensing, the innovative use of the ratio C/M is that it approximately cancels out the physical temperature while maintaining a high sensitivity to surface water change conveyed in the emissivity of the river [12]

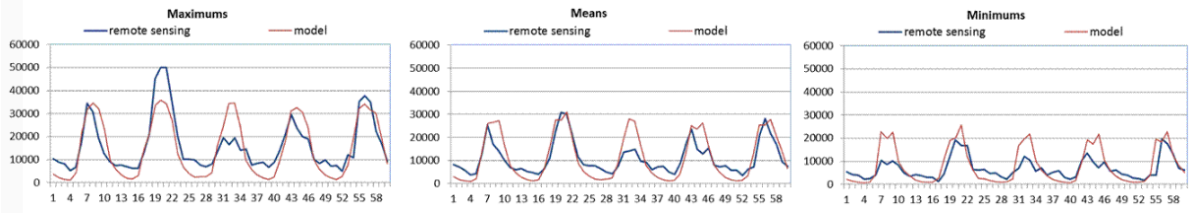

Figure 10. Same data as in figure 8, but arranged as time series of maximum (left) mean (middle), and minimum (right) discharge values. The red line shows the model results and the blue line is the remote sensing as transformed by the rating equation in figure 8.

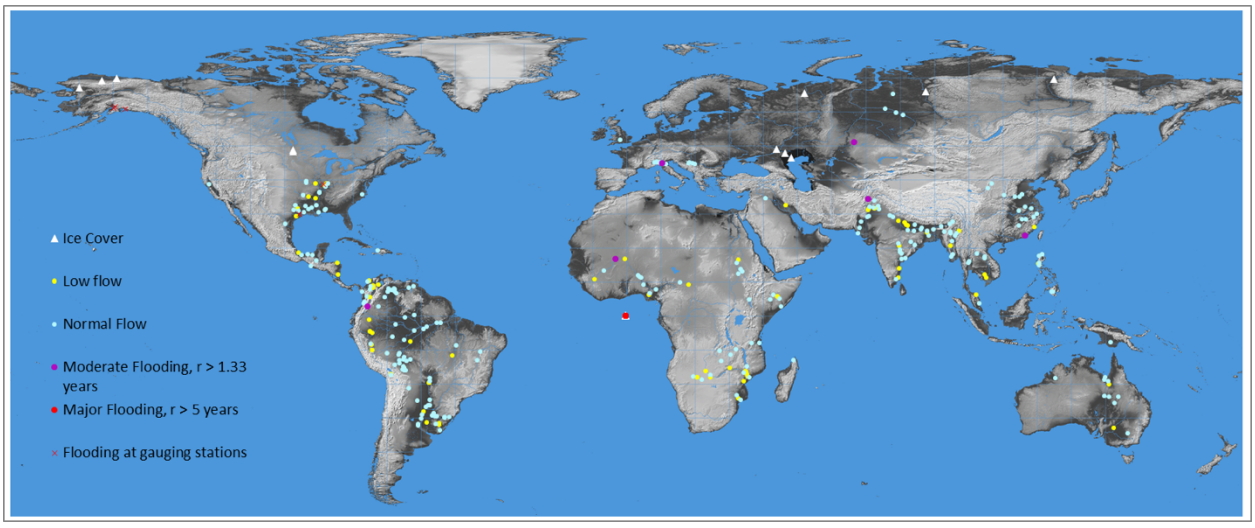

Figure 11. Status of River Watch version 3 online satellite gauging sites: Yellow dots for low flow, blue dots for normal flow, and purple (recurrence interval >1.5 y) and red (recurrence interval > 5 y) dots for moderate and severe flooding. Display is updated daily.

The sites within reach of TRMM (between 50o N and S) begin in January 1998, add AMSR-E data when such became available in mid-2002 (the data are merged), continue using TRMM only during the AMSR hiatus in 2012 and early 2013 (between AMSR-E and AMSR-2) and then extend to today using merged AMSR-2 and GPM. The record at higher latitude sites begins in mid-2002 (following launch of AMSR-E), and there is gap in 2012-2013 between the termination of AMSR-E and initiation of AMSR-2 because no data was collected at these locations for this interval (figure 12). The gridding algorithm to produce the global daily images is conducted at the Joint Research

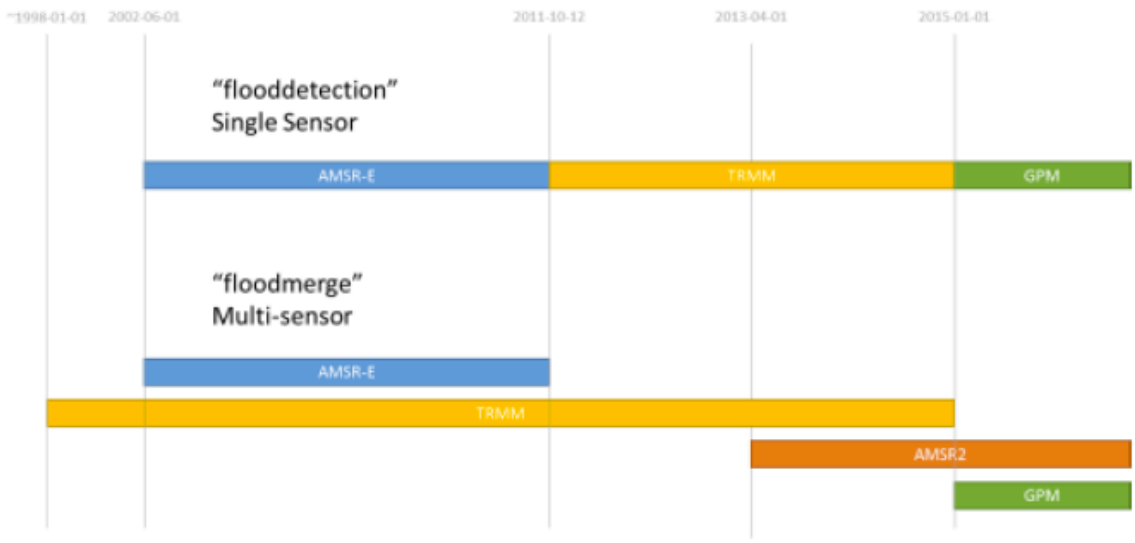

Figure 12. Temporal coverage, 1998 to present, of passive microwave sensors built and operated by NASA and by JAXA (Japanese Space Agency). Each satellite provides daily or near-daily imaging. Figure from [14].

Centre (JRC); the original data are near real time swath information from each sensor. A JRC document provides further information [14].

JRC produces a daily global grid at 10 km (near the equator) pixel resolution, and provides daily ratio data for fixed pixels within that 4000 x 2000 pixel grid. Where data from more than one sensor are available, the gridded product uses both [14]. At lower latitudes, the coverage is less than daily from AMSR-E and AMSR-2: River Watch Version 3.4 uses a forward moving 4-day running mean to avoid such data gaps and because river discharge exhibits strong temporal autocorrelation. At the JRC, all ratio values are calculated from values retrieved from near-real-time swath data products, and then projected in-house to the JRC grid.

At the Flood Observatory, the ratio data from the JRC are ingested once each day, and the html displays for each site are updated and added to the Observatory web site at 14:30 local time in Denver, Colorado, U.S.A. Each site outputs two html pages: one providing plots of the results but also some tabular data, the second, "data" html provides the rating curve and access to the complete record of satellite-measured discharge. For comparison purposes, a reference 20th percentile of the measured discharge for each day of the year, 2000-2010 is also calculated and provides a useful low flow threshold.

The River Watch approach to measuring river discharge is novel in that microwave sensors designed to monitor other aspects of the hydrologic cycle are here employed to measure river discharge changes and watershed runoff on the ground. Thus, in order to observe atmospheric conditions, such as precipitation, ground-sensing channels were included on AMSR, TRMM and now GPM: these provide the background component of upwelling microwave radiation against which precipitation can

be observed via other microwave frequencies. River Watch optimally uses just the ground-sensing channel, in particular the Ka-band channel, to avoid severe atmospheric effects compared to higher-frequency data; while retaining a better spatial resolution compared to lower-frequency data.

Discharge Measurement Accuracy

Several studies examine the impact of various ground characteristics on the accuracy of this microwave radiometry approach [15, 16]. As would be expected, there are locations where the method does not work well: 1) narrow straight, steep-gradient rivers where flow area expansion accommodates much less discharge variability than does velocity and depth, 2) channels with artificial levees that constrain all but rare floods from expanding onto the floodplain, 3) ephemeral rivers that flow only briefly after storm events, 4) rivers with heavily vegetated floodplains where tree canopies obscure the signal variation as flow area expands, and 5) ice-covered rivers, when ice cover is present (see section below). However, coupled with these constraints is the advantage that quite small rivers (usually meandering rivers), with channels of only a fraction of km in width, can be reliably monitored, provided that the gauging site chosen allows for flow expansion into channel/lower floodplain features: in-channel and side-channel bars, point bars (figure 5), small tributary mouths, and negative floodplain relief [17]. Braided rivers can also be measured through this approach, as these rivers strongly respond to discharge changes though flow area expansions and contractions. Also rivers even with steep banks, having large channels that contain sandbars and islands can be effectively monitored, even while *in situ* gauging methods may become inaccurate due to complex in-channel bathymetry and topography that are changing. Channel cross-sectional area at a gauging station is subject to excavation and aggradation even within a flood event; these changes have a less severe effect on rating curves when, instead, a 10 km long parcel of river and floodplain is being used to monitor discharge.

The combined remote sensing and model output also allow assessments of the signal to noise characteristics and the model to remote sensing agreement exhibited by each gauging site (table 1). As for *in situ* gauging stations, there is no expectation that each site records discharge changes with equal precision and accuracy. The *signal range* statistic records the total measured variability of the discharge-estimator signal; larger values indicate that the remote sensing signal is more sensitive to discharge variation. The *noise* statistic refers to the average signal variability, day to day: larger values indicate more non-hydrologic noises as even small rivers commonly do not vary greatly, *on the average*, between sequential days. Also, comparison to the model results provides useful information aside from the rating curve: the r^2 values, shown in the Table 1 examples, are the coefficient of determination of the remote sensing for the independent WBM modeling discharge results (over 5 years, 2003-2007). If the remote sensing is first calibrated to discharge values by the rating equation, these values are identical to those calculated via the Nash-Sutcliffe (N-S) equation [18].

The N-S statistic is often used to measure the predictive strength of hydrological models for actual measured discharge. In the present case, these values, for the global River Watch array, evaluate the predictive strength of the remote sensing as compared to the WBM global model results. This method commonly produces N-S values from .60 -.85. Also, as shown in figure 6, N-S and least squares coefficients of determination are sometimes much higher when the remote sensing is compared to *in situ* measured discharge rather than modeled discharge: the modeling is less accurate than the remote sensing.

Site	S/M	Range[1]	Range[2]	S/N	r^2
108	VG	.11	21	G	.66
23	G	.08	26	F	.57
26	VG	.09	17	F	.67
29	G	.12	36	F	.57
30	VG	.20	35	VG	.70

Table 1. Sample of microwave discharge (River Watch) measurement statistics at different sites along the Chindwin (108 and 23) and Ayeyarwady (26, 29, 30) rivers in Myanmar. Sites with high r^2 signal/model, "S/M" coefficient values suggest that both remote sensing and modeling are correlated and tracking actual discharge changes. Sites with larger signal range ([1]) and signal to noise (S/N) produce more stable daily values with smaller daily errors. Range[2] are discharge ranges between maximums and minimums observed in 10^3 m^3/sec. F, G, VG, and E criteria are described in text.

These descriptive statistics allow useful summary assessments of relative measurement site utility. Thus, a somewhat arbitrary but still meaningful ranking of how the gauging sites perform as compared to the model runs is as follows: r^2>.8, Excellent; >.7, Very Good; >.6, Good; >.44, Fair; <.44, Poor. Also, the S/N for all sites in the array can be assigned a ranking, as follows: >20, Excellent; >15, Very Good; >10, Good; >5, Fair; <5, Poor. Note that, in some cases, especially along large rivers, the n=180 model output, such as illustrated in figure 10, when compared to the equivalent time series of remote sensing signal, is apparently offset by one unit forward or backward in time, suggesting that the model routes the flow too quickly or too slowly to the measurement site. In this case, because the purpose of the modeling is to develop a rating curve, shifting the model output to match the remote sensing is appropriate and greatly improves the N-S and coefficient of determination statistics (e.g. from initial values such as .3 to shifted values of .7). This situation demonstrates the usefulness of the remote sensing information in the calibration of water routing and accumulation formulae and coefficients.

Detection of River Ice Cover

The initiation and removal of river ice cover can also be detected via microwave C/M information. Because the emissivity of water and soil is negatively correlated to the magnitude of the permittivity of water ε_w and soil ε_s respectively [13, 19] the C/M ratio changes from >1 to <1 when a river changes from the liquid to solid state, with the river permittivity magnitude switching from being larger to being smaller than that of soil as the river freezes up. This was demonstrated for the Lena River as a case study [12] For updated information, refer to [10, 20].

Figure 13 shows, from an earlier version of River Watch, the independent microwave signals obtained from a measurement pixel centered over an arctic river valley (River Watch site #100158, northern Pechora River, Russia) and from a pixel from adjacent land outside of the river valley. Figure 14 illustrates only the ratio data from the same site, for years 2014 and 2015, as transformed via a WBM-based rating equation and a filter applied to screen the ice-covered intervals. The filter automatically detects the dates in the spring and fall when the C/M data show minimum values, prior to the sharp rise as ice cover dissipates, and also just prior to re-establishment of ice and matching C and M in the fall.

In detail along river valleys, ice-break up and establishment can be complex. Ice jams may form and temporarily dam flow: producing backwater effects and disturbing the rating equation's validity. These processes can be examined in detail using optical sensors such as MODIS, but we use such data here to provide a simple validation of the microwave results. Shown in figure 15 are four sample MODIS scenes over this river reach during the 2014 spring and summer. They support the microwave signal independently obtained (figure 14).

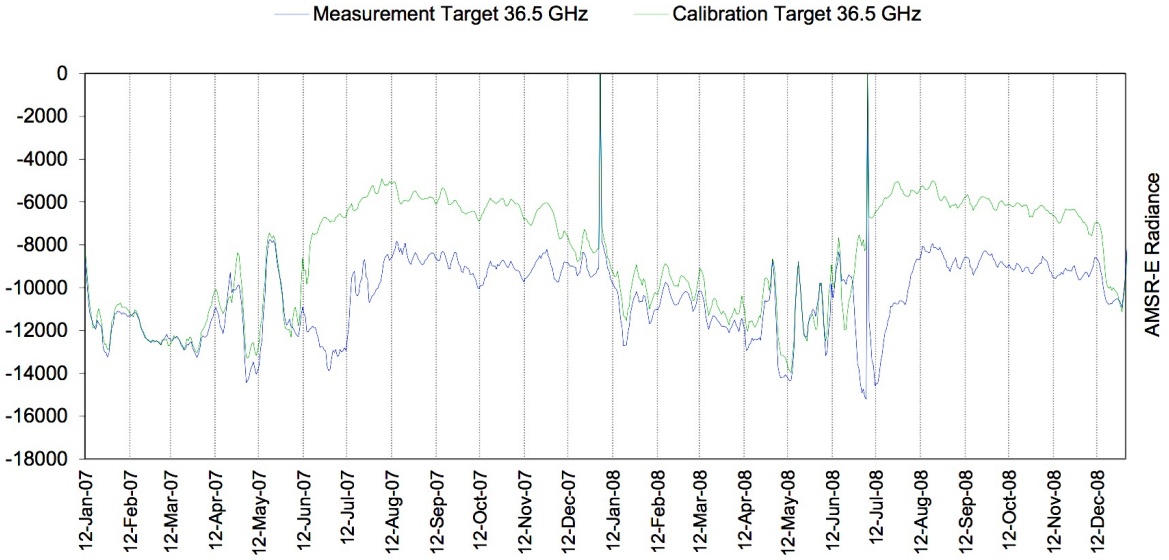

Figure 13. Brightness temperatures (digitized radiance values) measured by AMSR-2 for two years over River Watch site #100158 on the Pechora River, arctic Russia. The (lower) blue line, M shows data from the measurement pixel, over the river; the green line, C is from a near-by comparison pixel outside of the river valley. Transition to ice-free conditions occurs in latest May/early June (sharp drop in blue line); full ice cover is established by late December. The ratio C/M provides the discharge signal during the period without ice cover. Early summer high discharge progressively decreases during the mainly dry high arctic summer.

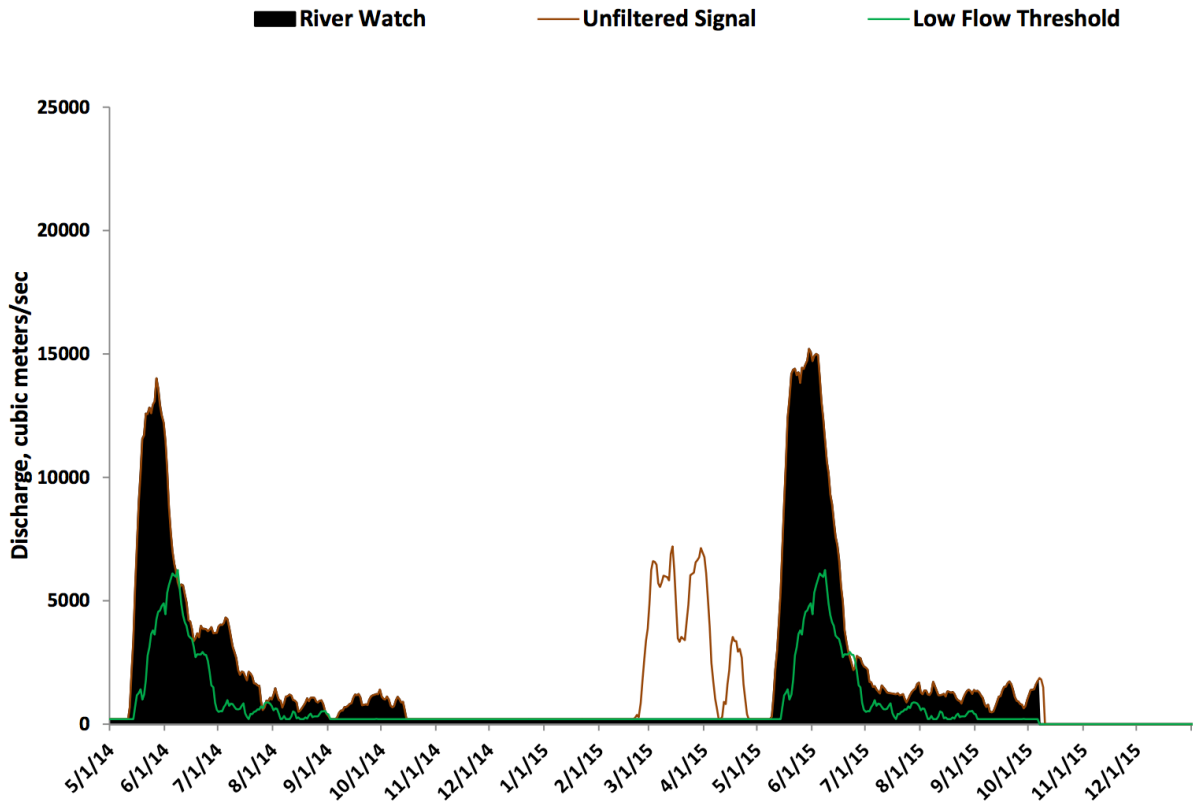

Figure 14. River Watch output for site #100158 showing two annual hydrographs, and the ratio signal prior to filtering (brown line) and after filtering (brown line underlain by black shading). Also shown is the 20th percentile discharge for each day used to identify unusually low flow or drought conditions (green line).

River Watch 3.4 uses source data processed at the Joint Research Centre that is provided only as C/M ratio information. Thus, the ice cover filter must detect ice-covered time periods using only the ratios. We locate the transition point in each season by determining the minimum ratio value within spring and autumn; the system then computes discharge values only between the times of these signal minimums. A constant sub-ice flow is estimated for the period of ice cover and from the modeling results. Figure 16 provides the monthly runoff time series at the Pechora River site; figure 17 shows the annual runoff values and changes in the ice-free season for each year. There is utility in maintaining such observations into the future for attempts to understand and monitor climate change in the Arctic, as excessive terrestrial heat flux into the Arctic Ocean via river discharge can impact sea ice retreat processes [21, 22].

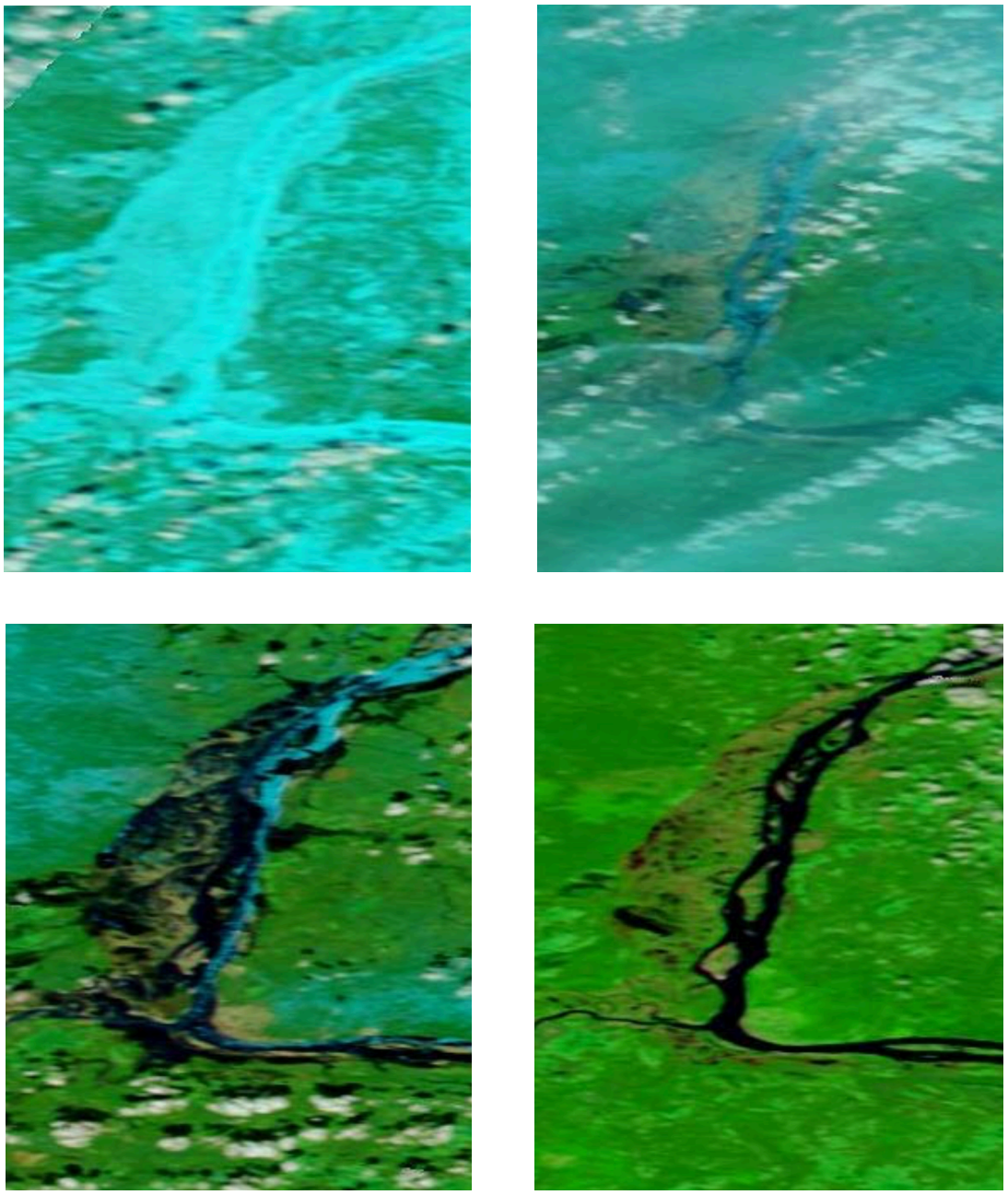

Figure 15. Four sample scenes from optical (MODIS bands 1,2,7) imaging of the Pechora River location used to provide visual confirmation of the timing of spring ice-out and following discharge changes. Compare with figure 14. Top left: May 4, 2014. Top right: May 14. Bottom left: May 16. Bottom right: June 17. According to these images, ice cover was fully in place still on May 4, but break-up was underway by May 14 (there is significant haze and cloud obscuration in this scene). Already by May 16, the flow area and discharge had greatly expanded: the "spring freshet" was underway. By June 17, the spring flood was already declining into the lower discharge values that would prevail for the rest of the summer.

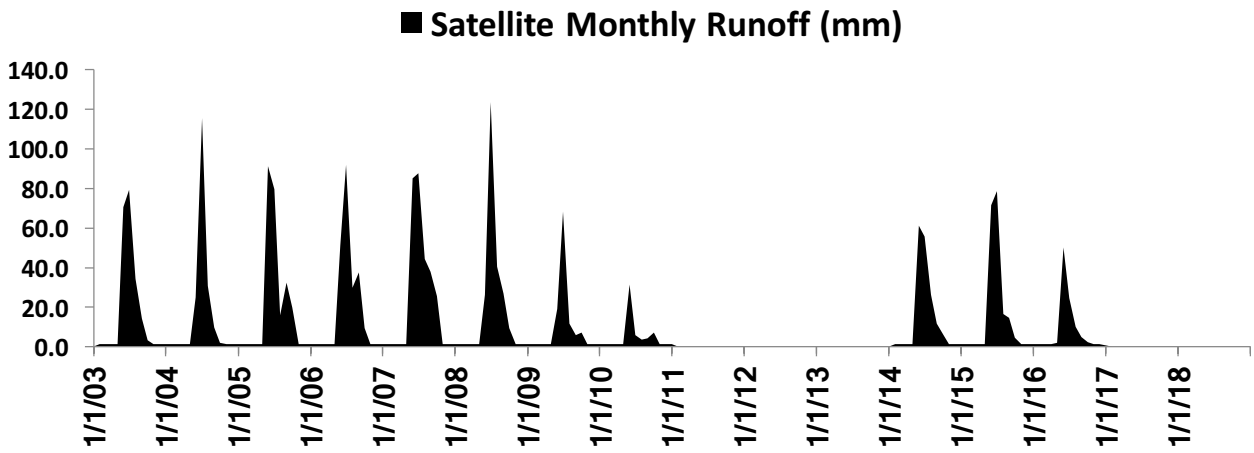

Figure 16. Monthly runoff for the Pechora River gauging site, showing low runoff amounts for 2010 but higher peak monthly runoff amounts for 2008 instead of 2007 (compare with figure 17). 2008 had a larger initial spring flood, but high discharge was sustained for a longer period through the summer in 2007. These data could also be examined to determine if unusually long seasons were caused by early ice release, late establishment of ice cover, or both.

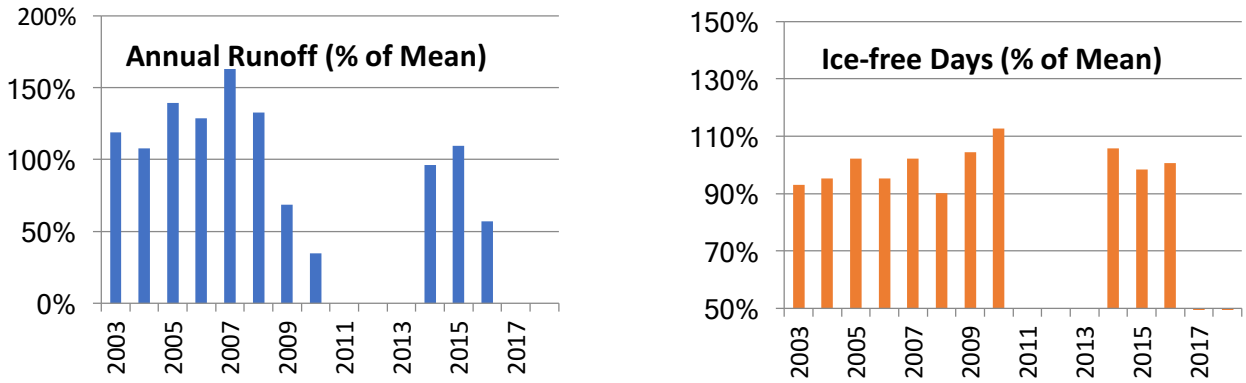

Figure 17. Total annual runoff at the Pechora River Watch site, upstream watershed area of 247,665 km^2 (left) and number of ice-free days (right), both expressed as percent of the mean. The year 2010 experienced an unusually long ice-free season, and also unusually low annual runoff. The year 2007 had unusually large total annual runoff during an ice-free season of normal length.

Summary and Conclusion

Passive microwave radiometry has surprising power to monitor river discharge changes at an appropriate temporal sampling interval and with considerable accuracy over multiple decades and continuing far into the future. This capability was unanticipated as the TMI, AMSR-E, AMSR-2, and GMI sensors aboard TRMM, AQUA, GCOM-W, and GPM and GPM satellites, respectively, were being designed. However, such measurements are key to water cycle assessments, and the demonstration we

and others have provided should spur further development of this capability, and incorporation into planning for future microwave satellite missions. Also, because of the continued maintenance of the pre-1998 37-GHz microwave records in data archives, and new processing techniques, the way is open for extending consistent river discharge and watershed runoff observational records back in time by at least another decade [23].

This paper notes several areas where current methodology is less than ideal, and more sophisticated methods of analysis could be employed. For example, signal to discharge rating curves are empirical in character, and should be created via flexible regression methods that allow the derived curves and equations to fit as closely as possible to the constraining data. Also, the discharge values are derived from imperfect global runoff models. Although these do have the advantage of being driven from observational precipitation amounts and land surface variables, it would be advantageous to develop a systematic method of comparing space-based to ground-based discharge measurements in order to detect model bias, and allow accurate extension of the ground-based data, even while accurate altimetry measurements from future satellites can be utilized as calibration data.

Finally, the microwave information also has the capability, in many cases, to automatically detect the timing and duration of ice-cover over high latitude rivers. The removal of ice cover is an important environmental/ecological variable throughout northern North America and Asia and over the Arctic Ocean, and the existing microwave sensors are sensing this variable. What remains is the work needed to process such data from many more measurement sites, link such to available ground sensors and other orbital data, and thereby provide important new information regarding arctic river freshwater discharge, terrestrial dissolved organic matter, and heat fluxes into the Arctic Ocean. This area of work is ready for rapid progress providing new measurement and analysis capabilities.

Acknowledgements

River Watch is a cooperative project between scientists at the University of Colorado, Boulder, CO, USA; at GDACS-GFDS (Global Disaster Alert Coordination System, Global Flood Detection System), European Commission Joint Research Centre, Ispra, Italy; at the University of Alabama; and at the Jet Propulsion Laboratory. R. Brakenridge acknowledges grant support from NASA. The research carried out at the Jet Propulsion Laboratory (JPL), California Institute of Technology by S. Nghiem, was supported under a contract with NASA, and in particular the work related to Arctic river discharge and ice cover at JPL was support by the NASA Cryospheric Sciences Program.

References

[1] B. M. Fekete, R. D. Robarts, M. Kumagi, H.-P. Nachtnebel, E. Odada, and A. V. Zhulidov, "Time for in situ renaissance," *Science,* vol. 349, no. 6249, pp. 685-686, 2015.

[2] A. I. Shiklomanov, R. B. Lammers, and C. J. Vorosmarty, "Widespread decline in hydrological monitoring threatens pan-Arctic research," *AGU Eos Transactions,* vol. 83, no. 13, pp. 16-17, 2002.

[3] J. S. Famiglietti, A. Cazenave, A. Eicker, J. T. reager, M. Rodell, and I. Velicogna, "Satellites provide the big picture," *Science,* vol. 349, no. 6249, pp. 684-685, 2015.

[4] B. M. Fekete, G. Pisacane, and D. Wisser, "Crystal balls into the future: are global circulation and water balance models ready?," *Proc. IAHS,* vol. 374, pp. 41-51, 2016.

[5] J.-F. Pekel, A. Cottam, G. N., and A. S. Belward, "High-resolution mapping of global surface water and its long-term changes," *Nature,* vol. 20584, 2016.

[6] D. Alsdorf, D., Lettenmaier, and C. J. Vorosmarty, "The need for global, satellite-based observations of terrestrial surface waters," *AGU Eos Transactions,* vol. 84, no. 269, pp. 274-276, 2003.

[7] G. R. Brakenridge, E. Anderson, S. V. Nghiem, and S. Chien, "Space-based measurement of river runoff," *EOS, Transactions of the American Geophysical Union,* vol. 86, 2005.

[8] Global-Runoff-Data-Center, http://www.bafg.de/GRDC/EN/Home/homepage_node.html, 2010.

[9] T. Pavelsky *et al.*, "Assessing the potential global extent of SWOT river discharge observations," *Journal of Hydrology,* vol. 519, pp. 1516-1525, 2014.

[10] G. R. Brakenridge *et al.*, "Calibration of orbital microwave measurements of river discharge using a global hydrology model.," *Journal of Hydrology,* vol. http://dx.doi.org/10.1016/j.jhydrol.2012.09.035., 2012.

[11] S. Cohen, A. J. Kettner, and J. P. M. Syvitski, "WBMsed: a distributed global-scale riverine sediment flux model - model description and validation. ," *Computers and Geosciences,* vol. doi: 10.1016/j.cageo.2011.08.011 (2011). 2011.

[12] G. R. Brakenridge, S. V. Nghiem, E. Anderson, and R. Mic, "Orbital microwave measurement of river discharge and ice status," *Water Resources Research,* vol. 43, no. W04405, doi:10.1029/2006WR005238, 2007.

[13] S. V. Nghiem *et al.*, "Microwave remote sensing of soil moisture – Science and applications, Chapter 9, part III," in *Remote Sensing of Drought – Innovative Monitoring Approaches*, vol. Drought and Water Crises Book Series: Taylor and Francis, 2012, pp. 197-226.

[14] T. De Groeve, G. R. Brakenridge, and S. Paris, *Global Flood Detection System Data Product Specifications* (JRC Technical Report.). Publications Office of the European Union, 2015.

[15] B. Revilla-Romero *et al.*, " 2015, On the use of global flood forecasts and satellite-derived inundation maps for flood monitoring in data-sparse regions. ," *Remote Sensing,* vol. 7, pp. 15702-15728, 2015.

[16] B. Revilla-Romero, J. Thielen, P. Salamon, T. De Groeve, and G. R. Brakenridge, "Evaluation of the satellite-based Global Flood Detection System for measuring river discharge: influence of local factors. ," *Hydrol. Earth Syst. Sci.,* vol. 18, pp. 4467-4484, 2014.

[17] J. Lewin and P. J. Ashworth, "The negative relief of large river floodplains," *Earth Science Reviews,* vol. 129, pp. 1-23, 2014.

[18] J. E. Nash and J. V. Sutcliffe, "River flow forecasting through conceptual models part I — A discussion of principles," *Journal of Hydrology,* vol. 10, no. 3, pp. 282-290, 1970.

[19] J. A. Kong, *Electromagnetic Wave Theory* Cambridge, Massachusetts: EMW Publishing, 2008.

[20] Z. Kugler and T. De Groeve, "The Global Flood Detection System," *EUR 23303 EN, Luxembourg: Office for Official Publications of the European Communities,* p. 45, 2007.

[21] D. Yang, X. Shi, and P. Marsh, "Variability and extreme of Mackenzie River daily discharge during 1973–2011 " *Quaternary International,* http://dx.doi.org/10.1016/j.quaint.2014.09.023., vol. 380-381, pp. 159-168, 2015.

[22] S. V. Nghiem, D. K. Hall, I. G. Rigor, P. Li, and G. Neumann, "Effects of Mackenzie River discharge and bathymetry on sea ice in the Beaufort Sea," *Geophys. Res. Lett.,* vol. 41, no. 3, doi:10.1002/2013GL058956, 2014.

[23] A. C. Paget, M. J. Brodzik, D. G. Long, and M. A. Hardman, "Bringing Earth's microwave maps into sharper focus," *Eos,* vol. 97, no. doi:10.1029/2016EO063675, 2016.